JOURNAL OF MATERIALS SCIENCE **36** (2001) 4089–4098

Effect of lanthanum-doping on the dielectric and piezoelectric properties of PZN-based MPB composition

W. Z. ZHU, A. KHOLKIN, P. Q. MANTAS, J. L. BAPTISTA
Department of Ceramic and Glass Engineering, University of Aveiro, UIMC, 3810-193 Aveiro, Portugal
E-mail: weizhong.zhu@pmusa.com

In this paper, effect of lanthanum doping on the dielectric and piezoelectric properties of the morphotropic phase boundary (MPB) composition in the $Pb(Zn_{1/3}Nb_{2/3})O_3$-$BaTiO_3$-$PbTiO_3$ system is presented. Samples were prepared according to the formula $Pb_{0.85-x}Ba_{0.15}La_x[(Zn_{1/3}Nb_{2/3})_{0.7}Ti_{0.3}]_{1-x/4}O_3$ ($0 < x < 0.3$), where the compensation for La ions was achieved via the appearance of B-site vacancies. All the compositions were synthesized using columbite precursor method and sintered using inverted crucible approach. Results of x-ray diffraction demonstrate that the solid solubility limit of La_2O_3 in the PZN-based MPB composition is more than 30 mole%. Incorporation of La_2O_3 into A-site sublattice of perovskite structure stabilizes rhombohedral phase against tetragonal phase, as a consequence, the location of the MPB composition range is displaced toward PT-rich end. In addition, the lattice distortion degree, represented by either tetragonality for tetragonal phase or rhombohedrality for rhombohedral phase, is reduced. Increasing La_2O_3 content remarkably decreases both the dielectric permittivity maximum and the temperature of the dielectric permittivity maximum. However, addition of La_2O_3 obviously strengthens the degree of the frequency-dispersion, which is correlated with the weakened degree of ferroelectric couplings among oxygen octahedra. The degree of diffuse phase transition (DPT) is prominently enhanced with increasing La_2O_3, for which the underlying mechanism is explored. Moreover, the ever-increasing extent of departure from Curie-Weiss behaviour induced by the lanthanum doping is indicative of some changes with the respect to the scale of polar microregions inherent to relaxors. The longitudinal piezoelectric coefficient (d_{33}) is maximized at 1 mole% La_2O_3, which is attributed to the combined effect of phase coexistence and enhanced contribution from non-180° domain wall process associated with rhombohedral phase.

1. Introduction

Lead zirconium niobate ($Pb(Zn_{1/3}Nb_{2/3})O_3$, designated as PZN) belongs to the family of lead-based relaxor ferroelectrics with different cations on the B-site of perovskite structure. It has a relatively high ferroelectric phase transition temperature being around 140°C at 1 kHz [1]. Compared to the normal ferroelectrics, the common features of relaxor ferroelectrics include diffused paraelectric to ferroelectric phase transition; higher dielectric permittivity value due to the extrinsic contribution of enhanced domain wall mobility; frequency-dependence of the dielectric permittivity and the temperature of the dielectric permittivity maximum (T_{max}) below Curie temperature (T_c). The temperature of the maxima in the dielectric constant shifts toward higher temperatures as the measuring frequency is increased whilst the dielectric loss exhibits the reversed behaviour [2].

Fabrication of pure perovskite-structured PZN ceramics is much more difficult, in comparison with its counterpart PMN, due to its inherently low tolerance factor. Hence, some amount of $BaTiO_3$ (BT) is usually intentionally added to promote the formation of perovskite phase, and as a result, preparation and characterization of the new PZN-BT solid solution system have been extensively studied [3, 4].

Modification of PZN-BT ceramics with $PbTiO_3$ (PT) is shown to decrease the relaxor characteristics in the dielectric response [5], namely, both the degree of the frequency relaxation characterized by the temperature difference of the dielectric permittivity maximum at different frequencies and the diffuseness coefficient of the ferroelectric phase transition at a fixed frequency are successively reduced with increasing PT content. For PZN containing 15 mole% BT, in analogue to the lead zirconate titanate (PZT) system [6], a morphotropic

phase boundary (MPB) where the rhombohedral and tetragonal phase coexist was found to fall into a broad composition region extending from 12 mole% PT to 18 mole% PT [7]. As with the PZT system, dielectric and piezoelectric properties of the compositions in the MPB region are maximized with the highest value occurring for the sample containing 15 mole% PT, which can be typically explained by the ease of domain reorientation due to the existence of multiple polarization directions inherent to both phases. Besides, it is also revealed that the improved dielectric and piezoelectric properties might be correlated with the enhanced domain wall mobility resulting from the minimization of the lattice distortion at MPB compositions.

Chen *et al*. [8] have reported an unusual microstructure in PMN by transmission electron microscope (TEM). They demonstrated the presence of short-range ordered domains on the scale of 2–5 nm, which were characterized by the presence of $\frac{1}{2}$ [111] superlattice reflections. It was further observed that the size of the these ordered regions did not coarsen on annealing at high temperature. They suggested that the ordering in mixed B-site cation relaxors was chemical in nature and the short-range ordered regions in PMN had a local Mg/Nb ratio of 1:1, as opposed to the global ratio of 1:2. Local charge imblance were then conjuctured to suppress coarsening, resulting in the stabilization of the short-range ordered domains. Donor doping like La^{3+} onto A-site was found to enhance the degree of ordering and the size of the ordered domains, giving further evidence supporting the possibility of this nonstoichiometrically-orderd nanoregions.

Lee *et al*. [9] studied the effect of lanthanum modification on the behavour of diffuse phase transition (DPT) and its underlying mechanism in PMN, and concluded that as a result of the enhancement of the 1:1 nonstoichiometric short-range ordering and the size of the domains in the presence of the excess of La_2O_3, the degree of the DPT was obviously increased. The substitution of La^{3+} for Pb^{2+} produces the positively charged Li_{pb} sites with a concomitant generation of electrons (electronic compensation mechanism), which expedites the growth of the negatively charged ordered nanodomains in a disordered matrix.

Effect of lanthanum doping on the degree of ferroelectric coupling is also well studied [10–12]. La modification (x) of $Pb(Zr_yTi_{1-y})O_3$(PLZT $x/y/1-y$) results in the destruction of long-range ferroelectric order. Rather, relaxor behaviour with a frequency dispersion of the dielectric response appears. Microscopically, with increasing La content, the sequence of domainlike structure evolves from normal micron-sized ferroelectric domains to precrusor tweedlike structure, finally to the polar nanodomains. The degree of relaxor behaviour in the PLZT is known to increase with increasing La content. It is believed that the coupling of ferroelectrically active oxygen octahedra is gradually weakened by the aliovalent La ions and resultant A-site vacancies. Above a critical lanthanum content (4 at% for rhombohedral PZT (65/35) and 12 at% for tetragonal PZT (40/60)), normal micrometer-sized ferroelectric domains cannot be sustained. For high-lanthanum-content compositions, sufficiently strong decouplings results in the stabilization of nanometer-sized local polar regions (polar nanodomains). Correspondingly, the macroscopic properties change from normal ferroelectric to relaxor ferroelectric types with increasing lanthanum content. Analogously, La modification of MPB compositions of PMN-PT was demonstrated to result in the evolution of polar nanodomains and relaxor characteristics from tweedlike structures [13].

The purpose of present work is to examine the effect of lanthanum doping on the phase constituents, dielectric and piezoelectric properties, degree of DPT and frequency dispersion of MPB compositions in the PZN-BT-PT system. For simplicity, the sample containing 15 mole% PT was chosen since it lies in the middle of MPB composition range and displays maximum dielectric permittivity and piezoelectric coefficient. Substitution of La^{3+} for Pb^{2+} is designed to be compensated by the introduction of B-site vacancies. It should be noted that due to the presence of B-site vacancies, the A:B site occupancy ratio for these compositions is more than 1.

2. Experimental procedure

Ceramic samples of various compositions in the La-modified $Pb_{0.85}Ba_{0.15}[Zn_{0.7/3}Nb_{1.4/3}Ti_{0.3}]O_3$ system were prepared. The raw powders were weighed according to the formula $Pb_{0.85-x}Ba_{0.15}La_x[(Zn_{1/3}Nb_{2/3})_{0.7}Ti_{0.3}]_{1-x/4}O_3$ ($0 < x < 0.3$) where the charge neutrality due to the aliovalent replacement is maintained by the presence of the negatively charged B-site vacancies. Columbite precursor method [14], in which ZnO and Nb_2O_5 were pre-reacted to form $ZnNb_2O_6$, was used in the present study to prepare the bulk ceramic sample. Specifically, raw materials of ZnO (>99% pure) and Nb_2O_5 (>99.5% pure) were weighed in mole ratio according to the stoichiometry of the chemical formula, ball-milled, dried, ground and calcined at 1000°C for 4 h in air with heating and cooling rates of 5°C/min. The calcined powders were ball-milled again for 6 h, dried, sieved and put in storage for subsequent usage. X-ray diffraction analysis confirmed that the calcined product was single phase $ZnNb_2O_6$.

Powders of La_2O_3 (>99.9%), $PbCO_3$ (>99% pure), $BaTiO_3$ (>99.5%), TiO_2 (>99% pure) and the previously prepared $ZnNb_2O_6$, were weighed in mole percentage according to the above-mentioned formula. To compensate for the PbO loss during the calcination and subsequent sintering, 5 wt% of excess $PbCO_3$ was incorporated. The mixture was ball-milled in a polyethylene jar for 12 h using yttria-stabilized zirconia balls and alcohol as milling media. The dried powders were ground again by pestle in an agate mortar for several minutes to break up some agglomerates. These powders were calcined at 900°C for 5 h in a covered alumina crucible with heating and cooling rates of 10°C/min. The calcined product was milled again for 6 h in the same way as described above for the mixing to reduce the particle size. The dried powders were sieved prior to

pressing. Pellets of 10 mm diameter and around 2 mm thick were obtained by uniaxial pressing at 100 MPa, followed by cold isostatic pressing at 300 MPa. Sintering was performed at 1150°C for 1 h with heating and cooling rates of 15°C/min. To minimise the lead loss, an inverted crucible method developed by Arkas *et al*. [15] was adopted. In this approach, the green pellets were placed in a larger crucible whose bottom was paved with a thin layer of the calcined powders. A smaller tight-fitting crucible was placed upside down on the bottom of the previous one and its surrounding was filled with $PbZrO_3$ plus PbO powders. Weight loss was less than 0.5 wt% after sintering and the relative density of the sintered samples measured by Archimedes' method was above 98%.

Phase identification and lattice calculation of the sintered samples crushed into powders were performed by X-ray diffraction analysis using Cu K_α radiation with a scanning speed of 1°/min and a stepsize of 0.02°. The relative fraction of the pyrochlore phase, if any, was calculated using the formula proposed by Swartz *et al*. [4]. For compositions containing both rhombohedral and tetragonal phases, partial overlapping of peaks belonging to two different phases at $2\theta = 45°$ on X-ray diffractograms often occurs. In order to calculate the relative fraction and lattice parameters of the two phases, the deconvolution of the ensembles of the peaks was performed to determine the angular position and integrated intensities of each peak. This was accomplished by fitting the parameters of the pseudo-Voigt functions to simulate the individual peaks to the diffraction patterns [16]. The relative fraction of rhombohedral phase was calculated using the following formula:

$$R\% = \frac{I_{r(200)}}{I_{r(200)} + I_{t(002)} + I_{t(200)}} \times 100\%, \qquad (1)$$

where $I_{r(200)}$, $I_{t(002)}$, and $I_{t(200)}$ refers to integrated intensity of the (200) plane of the rhombohedral phase, (002) and (200) planes of the tetragonal phase, respectively. Calculation of the lattice parameters was done by the least square approach using the angular position of each peak determined for two phases.

Samples for dielectric measurements were prepared by polishing parallel surfaces of the fired pellets with fine alumina sand paper, followed by sputtering gold electrodes and applying air-dried silver paint to improve electric contact. Dielectric measurements were carried out with an automated system, where a digital temperature controller connected with a tube furnace that was specially designed for the high temperature measurement and a Hewlett Packard 8248A LCR meter were controlled with a desk-top computer. Dielectric permittivities and dissipation factors were measured at various temperatures in the frequency range 0.1–100 kHz, as the samples were heated from low temperature to temperatures far above the transition range at a rate of 1°C/min. Measurements during cooling were also performed and no obvious difference between heating and cooling was found.

Piezoelectric charge coefficient, d_{33}, at room temperature was determined using Berlincourt Piezo d_{33} meter at 1 kHz (Model CADT, Channel Products, Chesterland, OH). Prior to measurement, specimens were poled in silicon oil bath during cooling from temperature far above T_m to room temperature and a dc bias field of 10 kV/cm was applied.

3. Results and discussion

3.1. Solid solubility limit of La_2O_3 in base composition $Pb_{0.85}Ba_{0.15}[(Zn_{1/3}Nb_{2/3})_{0.7}Ti_{0.3}]O_3$

XRD results (at room temperature) of the sintered ceramics in the $Pb_{0.85-x}Ba_{0.15}La_x[(Zn_{1/3}Nb_{2/3})_{0.7}Ti_{0.3}]_{1-x/4}O_3$ system for various compositions are illustrated in Fig. 1. It is found that only peaks of perovskite phase could be identified even for composition with 30% mole La_2O_3, no pyrochlore or other secondary phase was detected. This means that, within the resolution limit of XRD, the solid solubility limit of La_2O_3 in base composition via this compensation mechanism is higher than 30% mole. Such high level of substitution without appearance of secondary phase is not ever reported in the literature, to the knowledge of the author. It appears that B-site vacancy is a favourable defect species in this system. Chen *et al*. [8] once studied the domain evolution with the incorporation of La ions into PMN on A-site where the charge neutrality is maintained through the appearance of Pb vacancy. From TEM results, they observed that pyrochlore phase existed in the 5%mole-La-doped sample. They came to the conclusion that compensation for La^{3+} donor doping is achieved by adjusting Mg/Nb ratio via the formation of the pyrochlore phase, which is rich in Nb. Alternatively, lead vacancy is not a favourable defect species in this system.

In addition, effect of La^{3+} doping on the relative amount of rhombohedral and tetragonal phase was also determined from Fig. 1 using profile fitting. In adopting this approach, it is accepted that the integrated intensity ratio between (200) and (002) plane is 2:1 for tetragonal phase, and the (200) plane of rhombohedral phase usually coincides with (200) plane of tetragonal phase, leading to the broadening of diffraction profiles around $2\theta = 45°$ for compositions containing both rhombohedral and tetragonal phase. Presented in

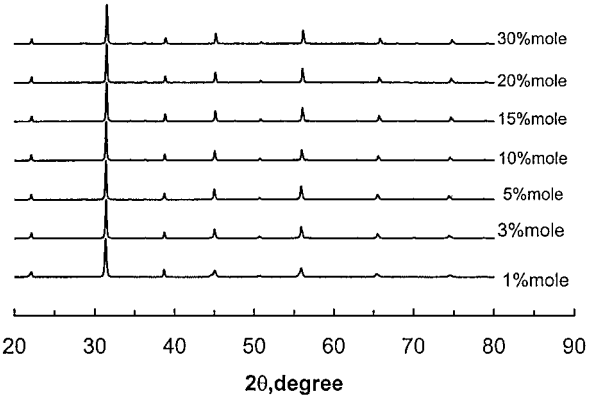

Figure 1 XRD patterns of La-modified PZN-based MPB compositions where the compensation for La is realized by the appearance of B-site vacancies.

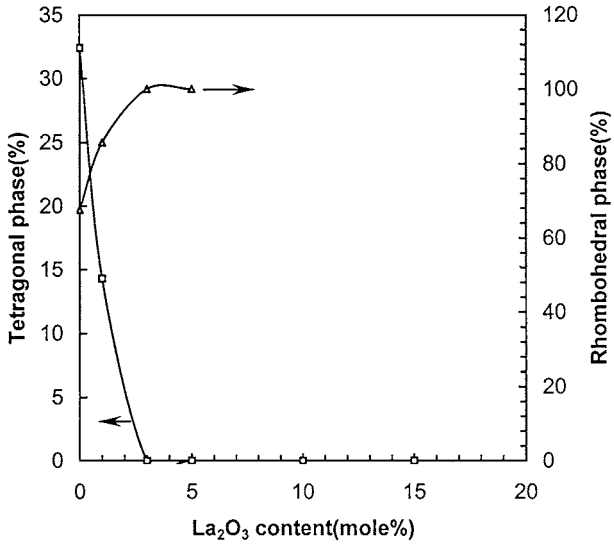

Figure 2 Effect of La-doping on the phase constituents of a series of samples composed of following compositions $Pb_{0.85-x}Ba_{0.15}La_x[(Zn_{1/3}Nb_{2/3})_{0.7}Ti_{0.3}]_{1-x/4}O_3$.

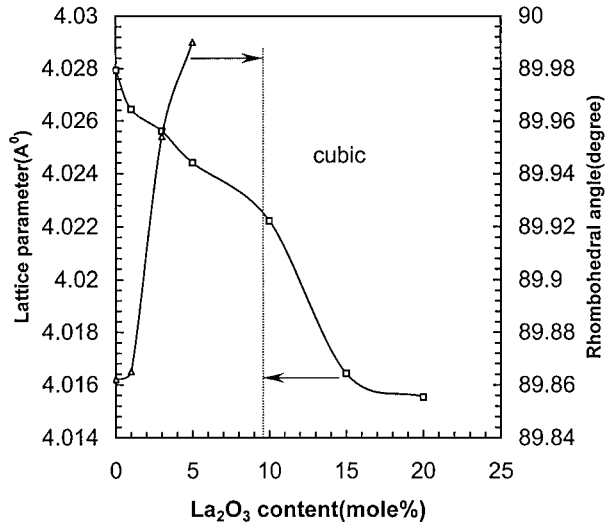

Figure 3 Effect of La-doping on the lattice parameter of the rhombohedral phase in the series of samples composed of following compositions $Pb_{0.85-x}Ba_{0.15}La_x[(Zn_{1/3}Nb_{2/3})_{0.7}Ti_{0.3}]_{1-x/4}O_3$.

Fig. 2 is the variation of relative amount of each phase with La_2O_3 concentration. Since the base composition is located in the middle of the MPB composition region, coexistence of rhombohedral and tetragonal phases is readily reflected in the XRD profile. With increasing La_2O_3 content, the relative amount of tetragonal phase dramatically decreases while that of rhombohedral (or pseduo-cubic) phase greatly increases. For doping level higher than 3% mole La_2O_3, the global symmetry is indeed single phase (either pseudo-cubic when T_m is higher than room temperature or cubic when the specimen is in the paraelectric phase region). Thermodynamically, incorporation of La ions into the lattice of perovskite structure stabilizes the rhombohedral phase against the tetragonal phase. In other words, addition of La_2O_3 shifts the MPB compositional region at room temperature toward high PT concentration end. This phenomenon is consistent with the experimental results for PLZT compositions close to MPB (53/47) where increasing the lanthanum content moves the structure from a long-range-ordered ferroelectric state having a low global symmetry to an average (pseduo) cubic structure having ordered polar regions with a lower local symmetry on the nanometer scale within an average cubic structure [15].

The lattice parameters of each phase for various compositions were calculated using the least square method after the deconvolution of peaks, and results for the rhombohedral phase are shown in Fig. 3. Tetragonal phase was found only in base material and 1%mole doped composition, and the value of tetragonality drops from 1.0108 to 1.0077 with the addition of 1%mole La_2O_3. Besides, for rhombohedral phase(irrespective of dual-phase and single-phase composition), the rhombohedral angle increases while the a-axis value decreases with increasing doping level. This indicates that the degree of lattice distortion, characterised by either tetragonality for tetragonal phase or rhombohedrality for rhombohedral phase, can be reduced by La_2O_3 doping with concomitant appearance of B-site vacancy.

3.2. Effect of La_2O_3 doping on the dielectric response

Profiles of relative dielectric permittivity and dielectric loss versus temperature at different frequencies for various specimens in the compositional series $Pb_{0.85-x}Ba_{0.15}La_x[(Zn_{1/3}Nb_{2/3})_{0.7}Ti_{0.3}]_{1-x/4}O_3$ where x is 0.01, 0.03, 0.05, 0.1, 0.15, and 0.2, respectively, are shown in Figs 4–9. Obviously, all the compositions

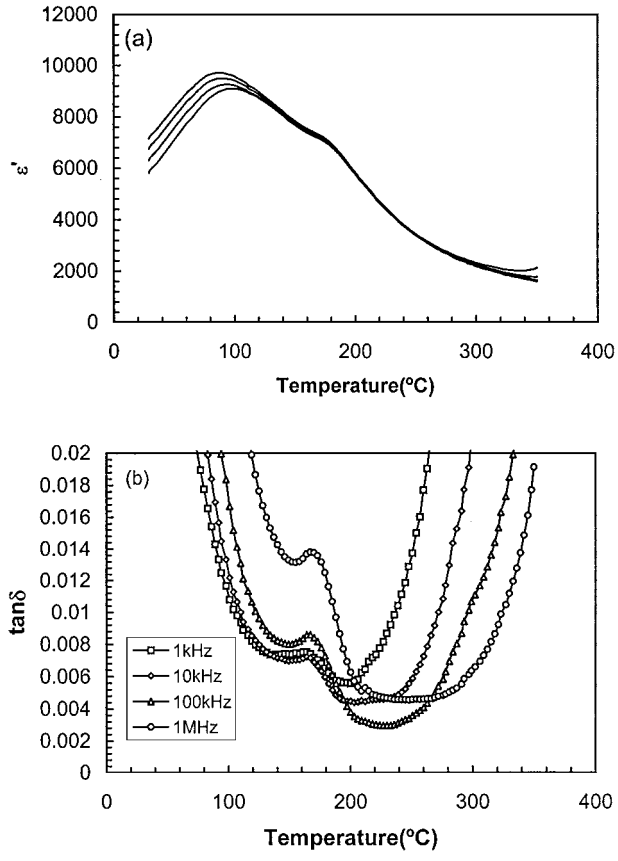

Figure 4 Relative dielectric permittivity (a) and dielectric loss (b) versus temperature for the 1 mole% La-doped specimen, the frequency for the permittivity value from the upper to low curve is 1 kHz, 10 kHz, 100 kHz, and 1 MHz, respectively.

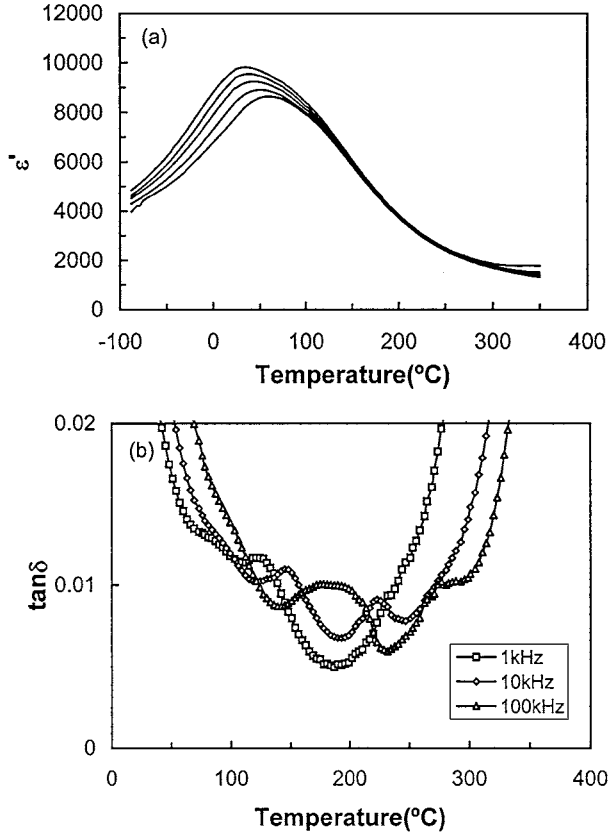

Figure 5 Relative dielectric permittivity (a) and dielectric loss (b) versus temperature for the 3 mole% La-doped specimen, the frequency for the permittivity value from the upper to low curve is 100 Hz, 1 kHz, 10 kHz, 100 kHz, and 1 MHz, respectively.

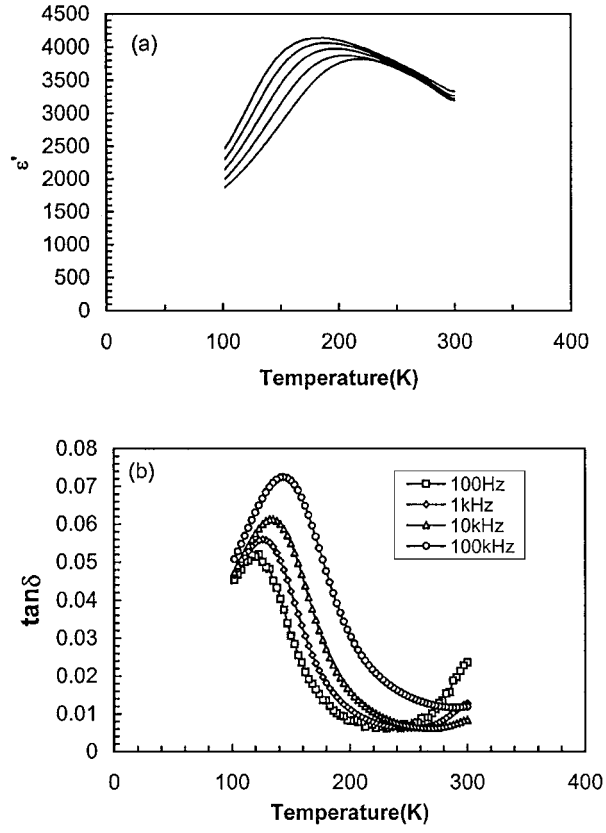

Figure 7 Relative dielectric permittivity (a) and dielectric loss (b) versus temperature for the 10 mole% La-modified specimen, the frequency for the permittivity value from the upper to low curve is 100 Hz, 1 kHz, 10 kHz, 100 kHz, and 1 MHz, respectively.

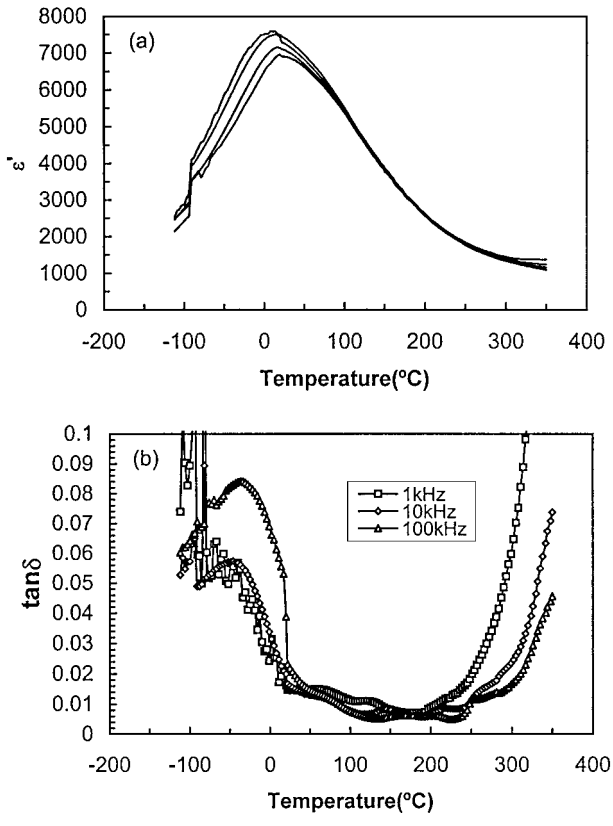

Figure 6 Relative dielectric permittivity (a) and dielectric loss (b) versus temperature for the 5 mole% La-doped specimen, the frequency for the permittivity value from the upper to low curve is 1 kHz, 10 kHz, 100 kHz, and 1 MHz, respectively.

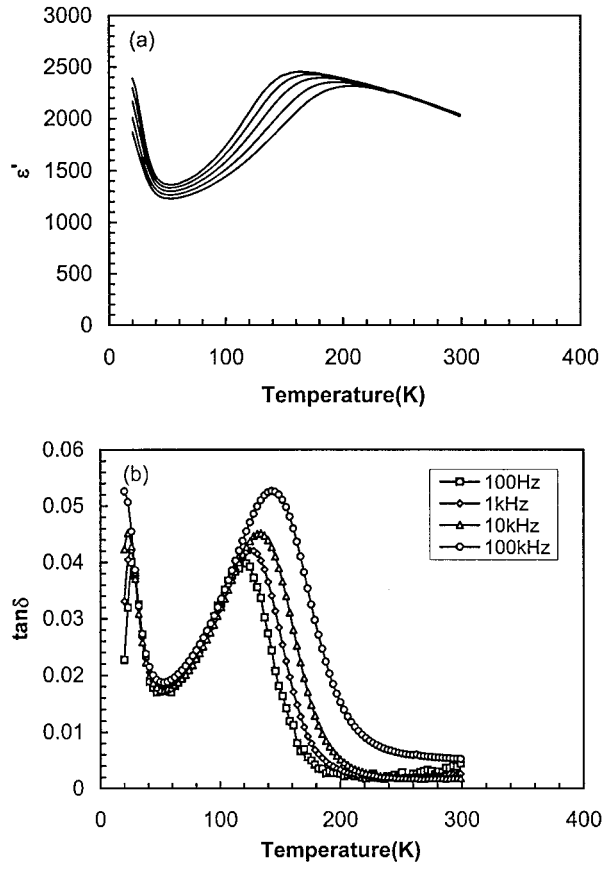

Figure 8 Relative dielectric permittivity (a) and dielectric loss (b) versus temperature for the 15 mole% La-modified specimen, the frequency for the permittivity value from the top to bottom curve is 100 Hz, 1 kHz, 10 kHz, 100 kHz, and 1 MHz, respectively.

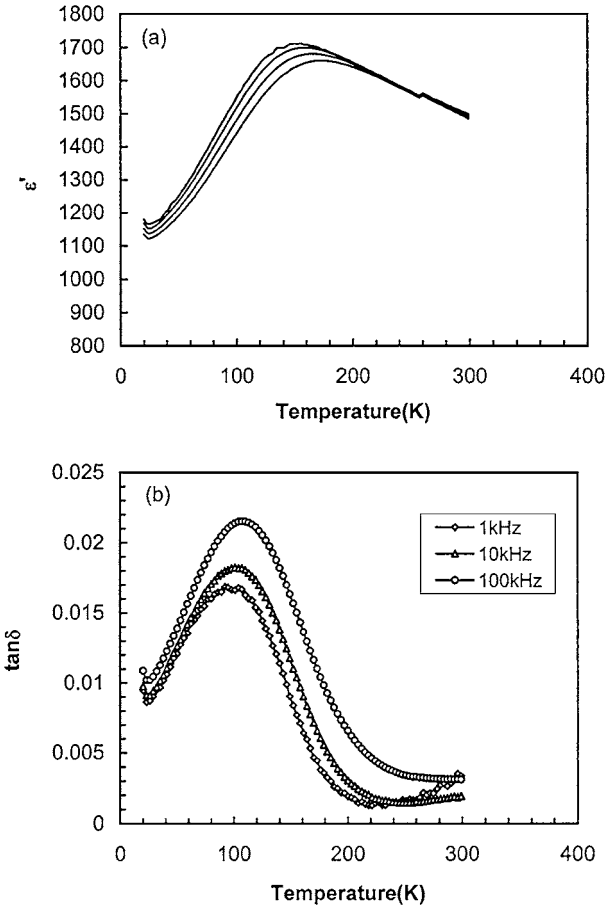

Figure 9 Relative dielectric permittivity (a) and dielectric loss (b) versus temperature for the 20 mole% La-modified specimen, the frequency for the permittivity value from the top to bottom curve is 100 Hz, 1 kHz, 10 kHz, and 100 kHz, respectively.

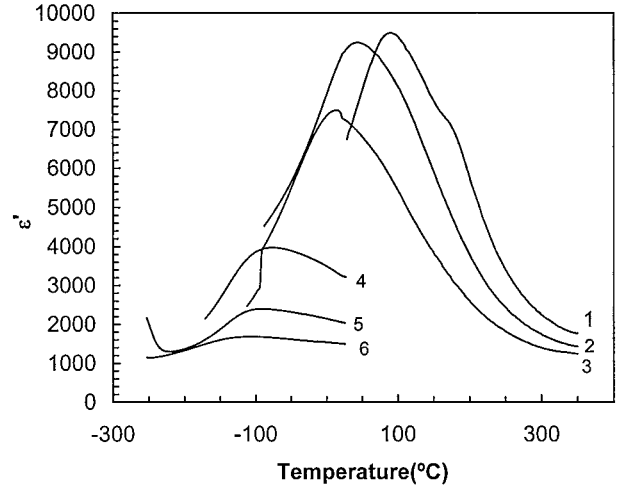

Figure 10 Relative dielectric permittivity versus temperature at 10 kHz for a series of samples composed of following compositions: $Pb_{0.85-x}Ba_{0.15}La_x[(Zn_{1/3}Nb_{2/3})_{0.7}Ti_{0.3}]_{1-x/4}O_3$, (1) $x = 0.01$; (2) $x = 0.03$; (3) $x = 0.05$; (4) $x = 0.10$; (5) $x = 0.15$; (6) $x = 0.20$.

exhibit typical ferroelectric relaxor behaviour, i.e. the paraelectric/ferroelectric phase transition extends over a broad temperature region (diffuse phase transition) in contrast with the sharp phase transition frequently observed in normal ferroelectrics; no macroscopic structural change is observed during this transition; the temperature of the dielectric permittivity maximum (T_m) shifts toward higher temperature while its value decreases as the measuring frequency is increased over several order of magnitude within the radio frequency range (100 Hz–100 kHz), the dielectric loss shows the reversed trend. As with PZT system, the incorporation of La ions into Pb-site apparently enhances the relaxor behaviour. Presence of more amount of excess La_2O_3 is inevitably associated with more pronounced relaxor behaviour.

To better illustrate the influence La_2O_3 doping on the dielectric response of the MPB composition, the relationship between dielectric permittivity and temperature measured at 10 kHz for this composition series is replotted as shown in Fig. 10. Evidently, addition of La_2O_3 moves DPT region toward lower temperature as well as significantly decreases the value of the dielectric permittivity. As a consequence, the value of dielectric permittivity at room temperature becomes relatively high and temperature insensitive for some compositions with adequate amount of La_2O_3 doping. The advantage is, when this relaxor ferroelectric is considered for potential application in the manufacture of multilayer ceramic capacitor (MLCC), which is one of the dominant application areas for relaxors, the value of room temperature capacitance is improved in conjunction with its reduced temperature coefficient. Besides, the composition with T_m slightly lower than room temperature is an ideal candidate for the application of electrostrictive transducers and actuators since the strain vs field response at room temperature is predominantly electrostrictive (induced strain proportional to the square of the applied electric field) rather than primarily piezoelectric (induced strain proportional to the applied electric field) such as base composition. For instance, the temperature of the dielectric permittivity maximum is 45°C for 1%mole doped specimen, which is slightly higher than room temperature. However, room temperature value of the dielectric permittivity is larger than that of the undoped specimen, hence, this composition is suitable for MLCC application given its enhanced DPT behaviour. On the other hand, T_m of the 3%mole doped specimen is slightly higher than room temperature and can be considered as electrostrictive material.

Fig. 11 shows the effect of La_2O_3 concentration on the peak value of dielectric permittivity at 10 kHz ($\varepsilon'_{\max 10\,kHz}$). When the doping level is smaller than 3%mole where the specimen contains both tetragonal and rhombohedral phases, decrease of $\varepsilon'_{\max 10\,kHz}$ with increasing the La_2O_3 content is modest. This can obviously be attributed to the enhanced ability for the polar nanodomains to follow the ac drive due to the maximisation of polarization directions inherent to two phases. On further increment of the La_2O_3 content, the relative dielectric permittivity maximum decreases significantly, which can be interpreted by the reduced directions of domain reorientation due to the appearance of the single phase. Additionally, the poor polarizability of La ions compared with that of Pb ions is also responsible for the very low $\varepsilon'_{\max 10\,kHz}$. It was reported that in La modified PZT with MPB composition, small amounts of lanthanum substitution

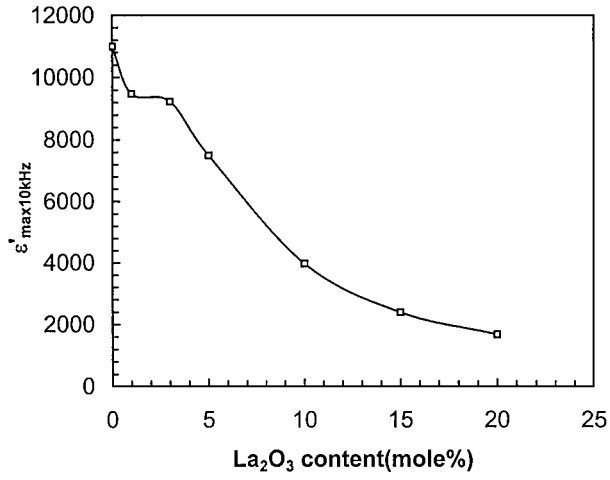

Figure 11 Effect of La_2O_3 concentration on the dielectric permittivity maximum at 10 kHz ($\varepsilon'_{\max 10\,\mathrm{kHz}}$) for the series of samples where the compensation for La is realized through the appearance of B-site vacancies.

(2 at.%) enhances the dielectric constant, switchable polarization, and field-induced strain [16]. The discrepancy between present results and those in PLZT probably stems from the microstructural difference. In our case, the base MPB composition already exhibits weak relaxor behaviour with polar nanodomain structure whilst the MPB PZT is a normal ferroelectric with micrometer-sized domain structure. Trace amount of La_2O_3 doping in PZT with MPB composition is considered to give rise to the enhanced domain reorientation.

Presented in Fig. 12 are variations of the temperature of the dielectric permittivity maximum at 10 kHz ($T_{\max 10\,\mathrm{kHz}}$) and the temperature difference between T_m at 1 kHz and 100 kHz ($\Delta T_1 = T_{\max 100\,\mathrm{kHz}} - T_{\max 1\,\mathrm{kHz}}$) that is usually employed to evaluate the degree of frequency dispersion for relaxors with the level of La_2O_3 doping. Qualitatively similar to the PZT system, $T_{\max 10\,\mathrm{kHz}}$ is drastically lowered by the incorporation of La_2O_3 into A-site of MPB composition. As expected, ΔT_1 increases monotonically with increasing doping level, indicating the enhanced degree of relaxor behaviour. It is well established that La modification

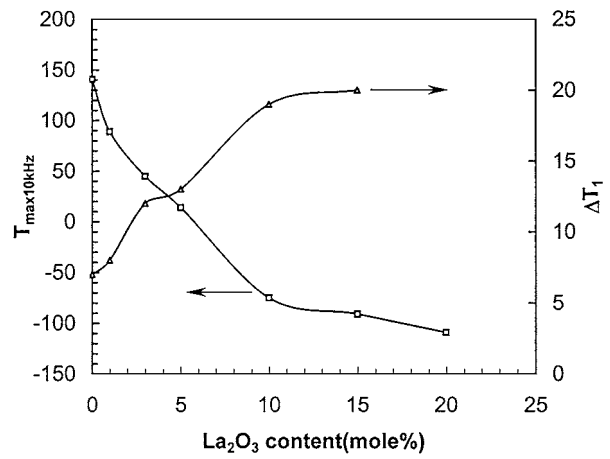

Figure 12 Variations of the temperature of the dielectric permittivity maximum at 10 kHz ($T_{\max 10\,\mathrm{kHz}}$) and the temperature difference between $T_{\max}$ at 1 kHz and 100 kHz (ΔT_1) with La_2O_3 content.

of PZT results in the destruction of long-range ferroelectric order, and above a critical lanthanum content, the frequency-dependent dielectric response with polar nanodomain microstructure develops. The degree of the relaxor behaviour is known to increase with increasing La_2O_3 content. The enhanced degree of frequency-dispersion in La modified MPB composition is believed to be associated with the weakened ferroelectric couplings among ferroelectrically active oxygen octahedra. It should be noted that in the case of PLZT, the compensation for the introduction of La ions into A-site is achieved by the generation of A-site vacancies rather than by the formation of B-site vacancies as in the present study. Therefore, presence of either A-site or B-site vacancy in lead-based perovskite ferroelectrics is likely to induce the relaxor behaviour via breaking the ferroelectric interaction and destroying the ferroelectric order.

3.3. Effect of La_2O_3 doping on the DPT behaviour

Not only the degree of relaxor characteristics, but also the width of diffuse phase transition (DPT) can be raised by increasing the La_2O_3 content. Shown in Fig. 13 is the change of the reduced dielectric permittivity $\varepsilon'/\varepsilon'_{\max}$ as a function of the reduced temperature $\tau = (T - T_\mathrm{m})/T_\mathrm{m}$ at 10 kHz for various compositions. It is visually explicit that the reduced dielectric response progressively becomes broader with increasing La_2O_3 concentration.

In the light of the compositional heterogeneity model proposed by Smolensky and Agranovskaya [17], the DPT can be explained on the basis of local compositional fluctuation on microscopic scales, resulting in a distribution of phase transition temperatures within the crystal. The underlying reason for the existence of microcompositional inhomogeneity in $Pb(B'_{1/3}B''_{2/3})O_3$-type perovskites is the development of its unique microstructure where the B-site 1:1 short-range-ordered nanodomains that is rich in B′ ions is embedded in

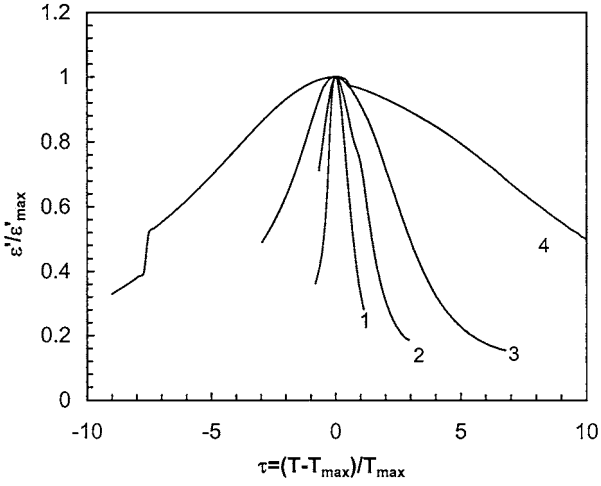

Figure 13 Plot of the normalized dielectric permittivity $\varepsilon'/\varepsilon'_{\max}$ against the reduced temperature $\tau = (T - T_{\max})/T_{\max}$ at 10 kHz for the series of the compositions composed of the following compositions: $Pb_{0.85-x}Ba_{0.15}La_x[(Zn_{1/3}Nb_{2/3})_{0.7}Ti_{0.3}]_{1-x/4}O_3$, (1) $x = 0.00$; (2) $x = 0.01$; (3) $x = 0.03$; (4) $x = 0.05$.

the matrix that is rich in B″ ions. In tandem with the evolution of this type of nonstoichiometric ordering, strong charge effect results, where the ordered microdomains have a net negative charge with respect to the disordered matrix. This charge imbalance is very effective in inhibiting the growth of domains even at high annealing temperatures, resulting in ultrafine micochemical domains approximately 2–5 nm in size in a disordered matrix composed of the polar microregions.

In reference to the previous study in La-modified PMN as well as the formula used for mixing, when the La ions are incorporated into the A-site sublattice of PZN-based MPB composition, the defect reaction process can be represented by the following equation, which is indeed an ionic compensation mechanism:

$$La_2O_3 \xrightarrow{3PbO} 2La^{\cdot}_{Pb} + 3O_o + V''_B \qquad (2)$$

Therefore, one can expect that, in ambient atmosphere, to maintain electron neutrality, the presence of positively charged $2La^{\cdot}_{Pb}$ is concurrent with the generation of negatively charged B-site vacancies. It is these positively charged $2La^{\cdot}_{Pb}$ defects that promote the charge compensation mechanism and expedite the growth of the negatively charged ordered nanodomains. As such, the degree of DPT is observed to increase with increasing La_2O_3 content due to the enhanced 1:1 nonstoichiometric short-range ordering.

One of the most salient features of ferroelectric relaxors, in general, is their pronounced deviation from Curie-Weiss behaviour at certain temperature interval above paraelectric to ferroelectric phase transition temperature, which is known to be associated with the average size and size distribution of polar microregions. It is cognisant that, in normal ferroelectrics, the Curie temperature (T_c) overlaps the onset temperature (T_{cw}) for spontaneous polarization indicating that the Curie-Weiss law is followed above T_c. Direct experimental evidence which supports this interpretation comes from the measurement of the temperature dependence of the refractive index $n(T)$ and strain $s(T)$ of ferroelectric relaxors. These results show that both $n(T)$ and $s(T)$ deviate from the expected linear temperature dependence of pure paraelectric behaviour and such deviations occur at temperatures far above T_m implying the existence of local polarization. Moreover, the dependence of the dielectric permittivity on temperature at $T > T_m$ can be described by the following empirical formula proposed by Uchino *et al.* [18].

$$1/\varepsilon' = 1/\varepsilon'_{max} + (T - T_m)^{\gamma}/C' \qquad (3)$$

where γ is a exponent in the range of 1.5–2, and C' is a parameter dependent upon the ε'_{max} and diffuseness coefficient.

Temperature-dependence of the dielectric susceptibility at 10 kHz for several typical compositions is depicted in Fig. 14, in which the onset temperatures for the deviation of Curie-Weiss response (T_{cw}) are

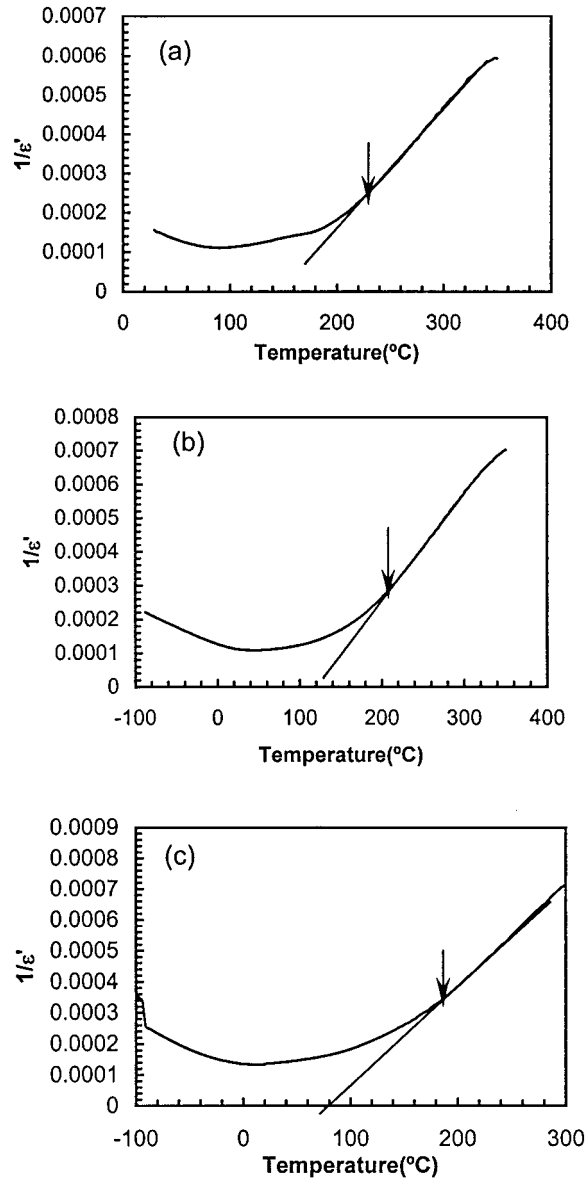

Figure 14 Temperature-dependence of the dielectric susceptibility at 10 kHz for several typical samples prepared according to the following formula: $Pb_{0.85-x}Ba_{0.15}La_x[(Zn_{1/3}Nb_{2/3})_{0.7}Ti_{0.3}]_{1-x/4}O_3$, (a) $x = 0.01$; (b) $x = 0.03$; (c) $x = 0.05$.

shown. Effect of La_2O_3 doping on the degree of deviation from Curie-Weiss law above T_m can be readily assessed by the temperature difference between T_m and T_{cw} at 10 kHz (designated as ΔT_2 hereafter) as illustrated in Fig. 15. With increasing La_2O_3 content, ΔT_2 was found to rise in spite of progressive decrease of T_{cw}. This implies that more amount of La_2O_3 doping is likely to result in the more pronounced degree of deviation from normal ferroelectric behaviour. As pointed out earlier, ΔT_2 can be correlated with the ease with which local polarization is induced. Heavy doping results in the readiness of the occurrence of polar nanodomains, contributing to the enhanced ΔT_2.

Illustrated in Fig. 16 is the frequency spectroscopy at $T = 0.9T_{max\,1\,kHz}$ for three doped samples. Apparently, increased doping leads to the enhanced frequency dependence of the dielectric permittivity, which can

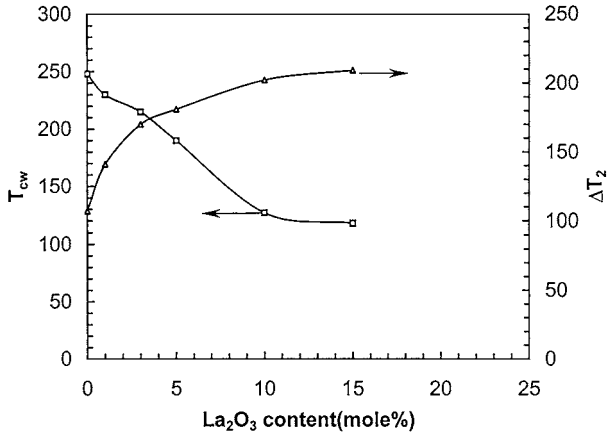

Figure 15 Effect of La_2O_3 content on the temperature at which the non-Curie-Weiss behaviour starts to occur (T_{cw}) and the temperature difference between the temperature of the dielectric permittivity maximum and T_{cw} at 10 kHz for the series of samples prepared according to the following formula: $Pb_{0.85-x}Ba_{0.15}La_x[(Zn_{1/3}Nb_{2/3})_{0.7}Ti_{0.3}]_{1-x/4}O_3$.

also be associated with broader size distribution of polar nanodomains.

3.4. Effect of La_2O_3 doping on the longitudinal piezoelectric coefficient (d_{33})

Fig. 17 shows the variation of d_{33} as a function of La_2O_3 concentration for La-modified MPB composition. In contrast with the dielectric permittivity maximum, the value of d_{33} is found to be maximized at 1 mol% La_2O_3, then it decreases sharply with increasing La_2O_3 concentration. It is well established that presence of multiple polarization direction arising from the coexistence of two phases allows the domain reorientation to be easily achieved, which qualitatively explains why the value of d_{33} of dual-phase composition is significantly higher than that of single-phase one. The slight improvement of d_{33} by the addition of 1 mol% La_2O_3 to the PZN-based MPB composition is most probably due to the shift of T_m close to room temperature that effectively activates part of large polar microregions that otherwise are "frozen in" in the undoped specimen, besides, the increased contribution from the non-180° domain wall movement

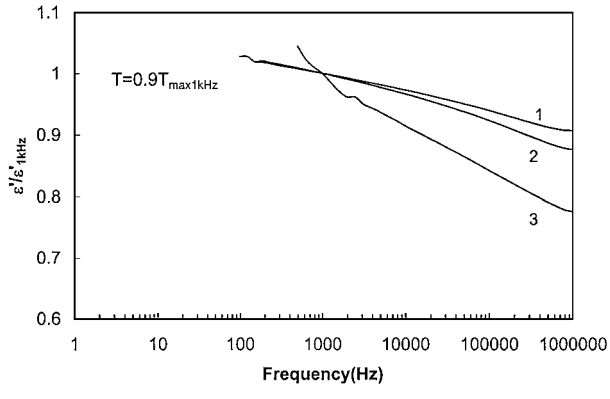

Figure 16 Frequency spectroscopy at $T = 0.9T_{max\,1\,kHz}$ for three compositions composed of following formula: $Pb_{0.85-x}Ba_{0.15}La_x[(Zn_{1/3}Nb_{2/3})_{0.7}Ti_{0.3}]_{1-x/4}O_3$, (1) $x = 0.01$; (2) $x = 0.03$; (3) $x = 0.05$.

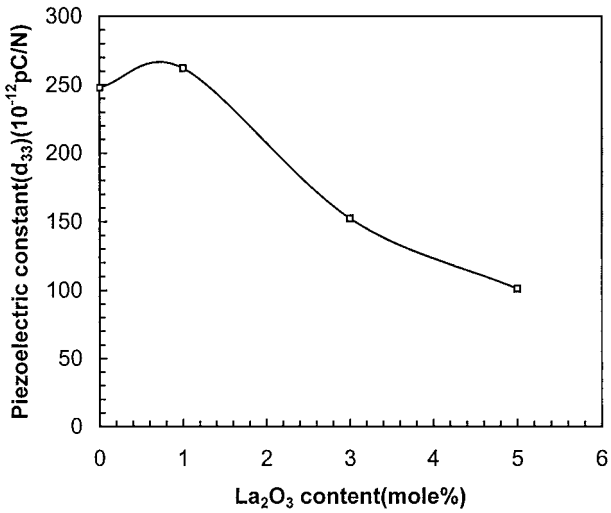

Figure 17 Effect of La_2O_3 content on the longitudinal piezoelectric constant of various samples composed of following compositions: $Pb_{0.85-x}Ba_{0.15}La_x[(Zn_{1/3}Nb_{2/3})_{0.7}Ti_{0.3}]_{1-x/4}O_3$.

associated with the rhombohedral phase is also important.

4. Conclusions

1. Solid solubility limit of La_2O_3 in the PZN-based MPB composition is higher than 30 mole% when the charge imbalance due to the substitution of La ions for Pb ions is compensated by the appearance of B-site vacancies. Incorporation of La_2O_3 stabilizes the rhombohedral phase against tetragonal phase, resulting in the shift of MPB composition range toward PT-rich end.

2. An increase of La_2O_3 content significantly reduces the dielectric permittivity maximum ($\varepsilon'_{max\,10\,kHz}$) as well as the temperature of the dielectric permittivity maximum ($T_{max\,10\,kHz}$) while enhances the degree of the frequency-dispersion. The dielectric properties of the two-phase compositions are generally superior to those of single-phase ones, which can be explained by the ease of domain reorientation due to the presence of multiple polarization directions inherent to both phases.

3. The degree of DPT behaviour can be profoundly promoted by La_2O_3 doping. This can be explained by the fact that the growth of the 1:1 nonstoichiometric short-range ordered nanodomains that is responsible for the compositional inhomogeneities and resulting DPT phenomenon is favoured since the negatively charged ordered regions are compensated by the positively charged defects.

4. The longitudinal piezoelectric coefficient (d_{33}) is maximized at 1 mole% La_2O_3. Coexistence of tetragonal and rhombohedral phase in combination with the enhanced non-180° domain wall processes inherent to rhombohedral phase contribute to this optimized value.

Acknowledgement

One of authors (W. Z. Zhu) is indebted to the Foundation for Science and Technologh (FCT) of Portugal for its financial support (PRAXIS XXI/BPD/16300/98).

References

1. J. KUWATA, K. UCHINO and S. NOMURA, *Ferroelectrics* **22** (1979) 863.
2. L. E. CROSS, *ibid.* **151** (1994) 305.
3. A. HALLIYAL, U. KUMAR, R. E. NEWNHAM and L. E. CROSS, *Am. Ceram. Soc. Bull.* **66** (1987) 671.
4. U. KUMAR and L. E. CROSS, *J. Amer. Ceram. Soc.* **75** (1992) 2155.
5. W. Z. ZHU, A. L. KHOLKINE, P. Q. MANTAS and J. L. BAPTISTA, *J. Mater. Sci*., submitted.
6. M. R. SOARES, A. M. R. SENOS and P. Q. MANTAS, *J. Europ. Ceram. Soc.* **19** (1999) 1865.
7. W. Z. ZHU, A. L. KHOLKINE, P. Q. MANTAS and J. L. BAPTISTA, *J. Amer. Ceram. Soc*., submitted.
8. J. CHEN, H. M. CHAN and M. P. HARMER, *ibid.* **72** (1989) 593.
9. K. M. LEE, H. M. JANG and W. J. PARK, *J. Mater. Res.* **12** (1997) 1603.
10. X. H. DAI, Z. XU, J. F. LI and D. VIEHLAND, *ibid.* **11** (1996) 626.
11. Q. TAN and D. VIEHLAND, *J. Appl. Phys.* **81** (1997) 361.
12. X. H. DAI, Z. XU, J. F. LI and D. VIEHLAND, *J. Mater. Res.* **11** (1996) 618.
13. S. M. GUPTA and D. VIEHLAND, *J. Amer. Ceram. Soc.* **80** (1997) 477.
14. S. L. SWARTZ and T. R. SHROUT, *Mater. Res. Bull.* **17** (1982) 1245.
15. S. M. GUPTA, J. F. LI and D. VIEHLAND, *J. Amer. Ceram. Soc.* **81** (1998) 557.
16. J. F. LI, X. H. DAI, A. CHOW and D. VIEHLAND, *J. Mater. Res.* **10** (1995) 926.
17. G. A. SMOLENSKII, V. A. ISUPOV, A. I. AGRANOVSKAYA and S. N. POPOV, *Sov. Phys. Sol. Stat.* **2** (1961) 2584.
18. K. UCHINO and S. NOMURA, *Ferroelectr. Lett.* **44** (1982) 55.

Received 9 October 2000
and accepted 4 May 2001